

EXPERIMENTAL TESTS OF A PROTOTYPE SYSTEM FOR ACTIVE DAMPING OF THE E-P INSTABILITY AT THE LANL PSR*

C. Deibele, S. Assadi, S. Danilov, S. Henderson, M. Plum, ORNL, Oak Ridge, Tennessee
 D. Gilpatrick, R. McCrady, R. Macek, J. Power, T. Zaugg, LANL, Los Alamos, New Mexico
 J. Byrd (LBNL, Berkeley, California), S. Breitzman, S. Y. Lee, IU, Bloomington, Indiana
 M. Pivi, SLAC, Menlo Park, CA
 M. Schulte, A. Poliseti, Z. Xie, UW Madison, Madison, WI

Abstract

A prototype of an analog, transverse feedback system for damping of the two-stream (e-p) instability has been developed and successfully tested at the Los Alamos Proton Storage Ring (PSR). This paper describes the system configuration, results of several experimental tests and studies of system optimization along with studies of the factors limiting its performance.

INTRODUCTION

The PSR (proton storage ring) in Los Alamos has undergone many studies over its lifetime and it has been observed to undergo an e-p instability for various machine configurations. This e-p instability is of particular interest to the SNS (Spallation Neutron Source) in Oak Ridge as the beam intensities and beam power are significantly higher than at PSR, while the machine configurations are somewhat similar.

The physics behind the e-p instability are shown pictorially in Figure 1.

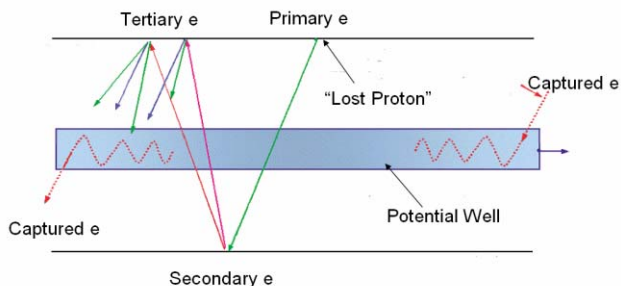


Figure 1: A diagram describing the e-p instability. Picture by Pivi.

Electrons that sit in the beamline are accelerated into the potential well of the proton bunch as the proton beam passes. As the proton beam leaves, the electron gains energy and strikes a beampipe wall creating secondary electrons. The secondary electrons undergo the same process and soon the proton beam begins to oscillate from space charge becoming unstable causing losses to occur.

Various studies [1-4] have shown that the e-p instability is wideband and therefore it was envisioned to use a wideband feedback system to stabilize the proton beam in

the ring. An analog system was developed and deployed at PSR to study damping and system effectiveness.

A model and some results of the wideband feedback system were described in [5], and new progress in system design is presented in this paper.

ANALOG SYSTEM DESCRIPTION

A schematic of the deployed analog feedback system is shown in Figure 2. A description of each component follows.

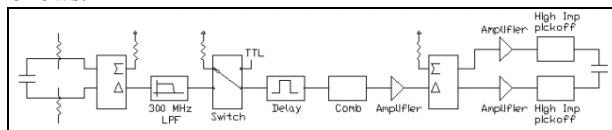


Figure 2: Schematic of wideband feedback system [5].

In Figure 2, the signals flow from left to right. The vertical beam position signals are picked up using stripline pickups. The signals are conditioned using fixed attenuators so that the resulting difference is minimized for a stable beam, or the beam lies on the electrical axis of the pickups. Next, the signals go through a 180 degree hybrid, and the resulting signal is proportional to both beam intensity and position.

Bandwidth Considerations and Power Amplifier

The next component is a low pass filter, which is necessary because the high power amplifiers (ENI 5100L) have dispersion [6]. A measurement of the dispersion is shown in Figures 3-4 [5].

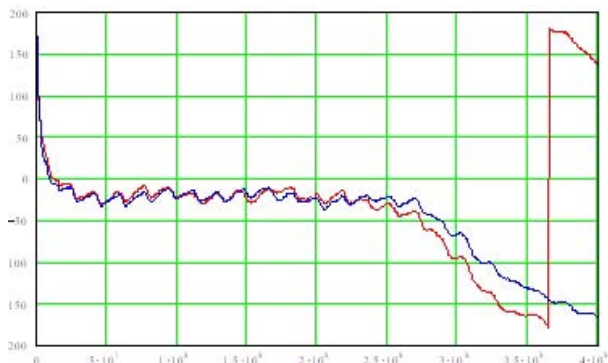


Figure 3: The unwrapped phase of the power amplifiers begins to have phase dispersion at about 300 MHz.

* ORNL/SNS is managed by UT-Battelle, LLC, for the U.S. Department of Energy under contract DE-AC05-00OR22725

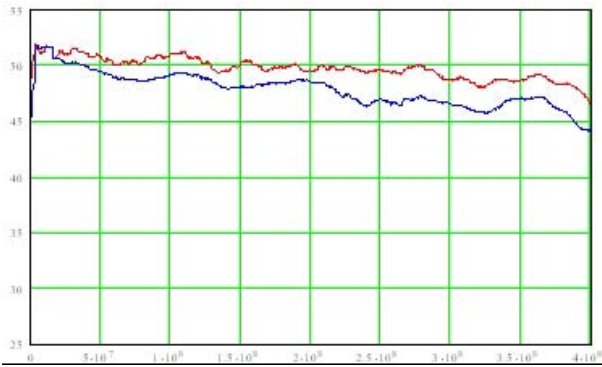


Figure 4: Magnitude of transfer function of high power amplifiers.

Since it is the real part of the signal that does the actual damping, phase dispersion plays a significant role in system design considerations. It is essential therefore to attenuate the system for frequencies where the phase dispersion will cause positive feedback.

TTL RF Switch and Low Level Amplifier

Next, a low power high speed switch (Minicircuits ZYSWA-2-50DR) is used so that the LLRF system can be turned on or off at various times during accumulation or store to study the growth rate of the instability and to measure the damping rate of the feedback system. Low-level amplifiers and step attenuators were used to fine-tune the gain of the overall system so that it can be optimized for various machine configurations.

Delay Line

The length of the delay line is a function of the tune of the particular ring. At PSR, it was necessary to have a total delay of four turns, or about one microsecond. This is a long delay, and using coaxial lines to accomplish this delay would have caused both loss as well as dispersion. It was decided, therefore, to use a fiber-optic technology for the majority of the delay, and use a series of binary switches to fine-tune the delay.

The fiber optical delay was designed with the goal of system flexibility in mind, and therefore an operator-switchboard style of choosing delays was designed. Steps of 10 nanoseconds for up to 50 nanoseconds and then steps of 50 nanoseconds up to 1 microsecond can be easily selected. A picture of the fiber optic delay box is shown in Figure 5. [5]

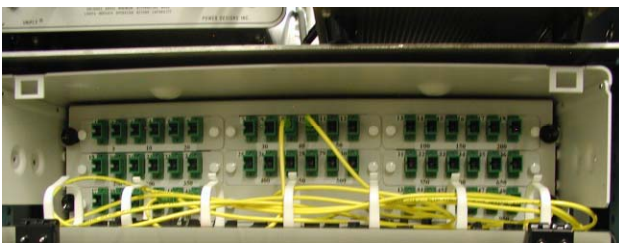


Figure 5: Operator-style adjustable delay fiber optic delay box.

The binary delay section was manufactured using coaxial lines and TTL-switches. Each switching section increased delay in binary increments from 200 picoseconds to 12.8 nanoseconds. This permitted the user to adjust and tune the system delay quickly without having to reconfigure any analog electronics. A schematic picture of a binary delay section is shown in Fig. 6. [5]

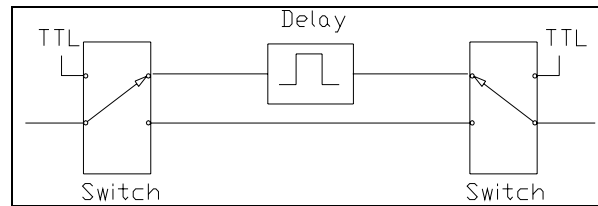


Figure 6: Schematic of binary delay section. These delays are cascaded together with each section having increasing delays.

Comb Filter

Many discussions about the choice of comb filter configuration drove the desire to have a flexible comb filter. Four different comb filter configurations were designed with two being available at any one time. Again, since the delay of the comb filter is a function of the ring frequency, and at PSR the delay is about 358 nanoseconds, it was decided to use fiber optic technology. A schematic of the comb filter is shown in Figure 7. [5]

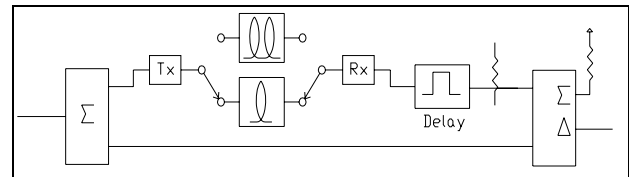


Figure 7: Schematic diagram of the comb filter.

Here, one can either choose a single turn of delay or two turns of delay. A fine-tune adjustment using a trombone section is chosen to align the notches, and an attenuator is used to optimize the notch depths. Two of these comb filters were deployed so that one can cascade the filters to test different machine configurations. A picture of the comb filter chassis is shown in Figure 8. [5]



Figure 8: Comb filter chassis.

The resulting measurement of the comb filter showed that notches of up to 50 dB are achievable, with each filter having about 30 dB notch depths. Measurement of the cascaded comb filters is shown in Figure 9.

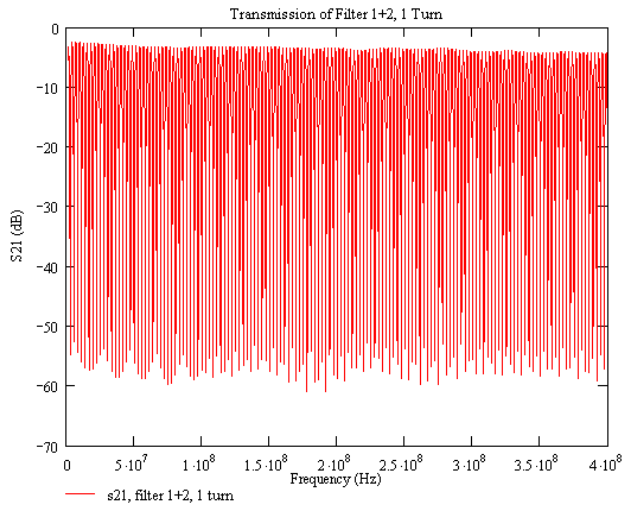


Figure 9: Transmission measurement of two notch filters with a single turn in the long leg.

High Impedance Pickoff

During operations, it is desired to measure the signals that are sent to the kicker stripline electrodes. A simple high-impedance pickoff was designed and implemented to make this measurement. A sample circuit picture is shown in Figure 10.

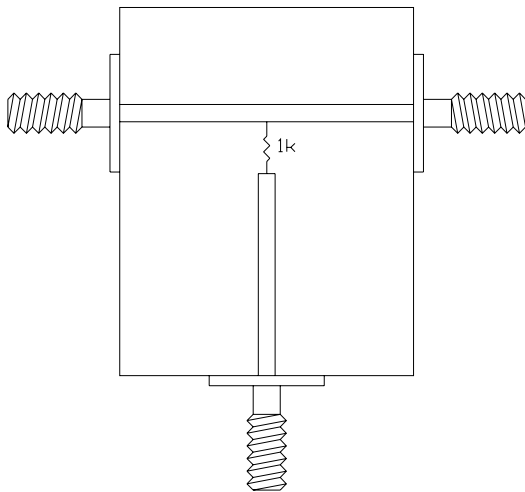
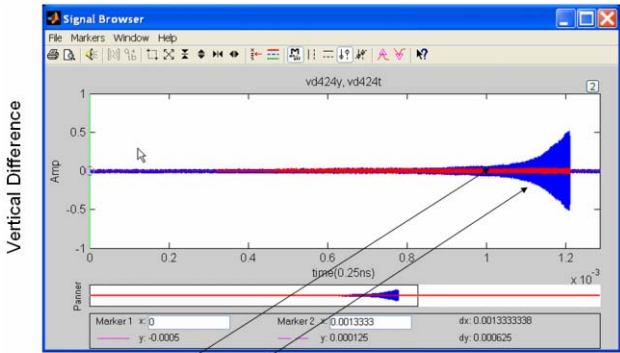


Figure 10: High impedance pickoff circuit.

SAMPLE MEASUREMENT RESULTS

Sample measurements showing the performance of the analog feedback system follow. In Figure 11 the feedback system shows it is possible to damp e-p with a wideband feedback system. The red trace shows the vertical difference signal when the feedback system is on, the blue trace shows the vertical difference signal when the feedback system is off. Each case has the same stored charge and buncher voltage.



FB ON, FB OFF 3 μC/pulse, buncher 5.0 kV

Figure 11: Picture courtesy of R. Macek.

Figure 12 shows the evolution of the instability with respect to time. The turn axis is time as measured by turns of beam around the ring. The mode axis is bins of signal in the frequency domain and normalized to harmonic frequency of the beam revolution frequency around the ring. An FFT of the signal is then performed as a function of time and is plotted on the vertical axis.

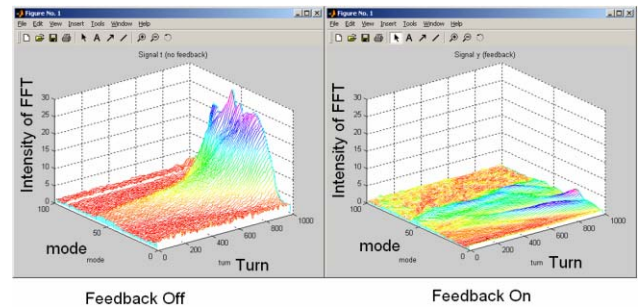


Figure 12: The turn axis is equivalent to time, and the mode axis is an FFT of several turns of data, showing the bandwidth of the instability and performance of the feedback system. Photo courtesy of Breitzmann.

The first set of measurements showed that the feedback system was capable of reducing the threshold of instability, as measured by the buncher rf system, by 10%. After more beam studies, the experimental improvement on the damper system demonstrated a peak reduction in threshold by about 30%.

ANALOG SYSTEM PERFORMANCE ISSUES

Measurements on the system performance during beam study periods have shown that several limitations on the analog system exist. A brief discussion of these performance issues follows.

First, the analog system is limited by power. A different set of pickup and kicker electrodes could be deployed which would more efficiently couple to the beam in the bandwidth of interest.

Next, the high power electronics need to be upgraded to be able to do drive about 400 Watts on each electrode. Currently we are limited to 100 Watts.

Designing and building an equalizer to force the phase to be zero in the system would automatically improve system performance, as the phase of cables + electronics is about 20 degrees across the band. This translates into a power loss of about 10%.

We were not able to see an improvement in the performance of the system with the comb filters deployed. There are several reasons that could cause this behavior.

- The fiber transmitters may be in compression and cause the filter to misbehave.
- The hybrids have good isolation, but they are not perfect. Adding a unity gain amplifier on the short leg may force that any leakage due to the hybrid to not contaminate the long leg.
- The notch spacing of the comb filter may not be spaced correctly. An external 10 MHz source was used to lock the network analyzer, but it may not have been synchronized properly with the ring RF.
- Discussions about the use of single or double turns in the long leg are still ongoing and time is needed to determine which is ideal for the PSR.

FUTURE WORK

The University of Wisconsin Madison Electrical Engineering department has joined the collaboration in studying e-p. A mixed signal system to improve performance and flexibility in the system is being developed. The goal of this system is to be able to run the system at a full duty cycle, save data for offline analysis, and to permit the system to be able to run in a ramped frequency mode. The new system simply replaces a part of Figure 2 with an FPGA based system. The parts in Figure 13 in the red box are now to be replaced with a digital control algorithm.

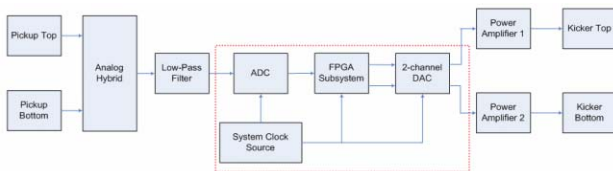


Figure 13: Mixed signal feedback system. The part in red is an FPGA based digital control system.

This new system design uses a single clock source that is provided externally and is running at a harmonic of the ring RF clock. To prevent aliasing, this harmonic must be higher than the Nyquist frequency of the highest harmonic that is present in the instability spectrum. Using a harmonic of the ring RF system ensures also that a simple algorithm for the comb filters can be deployed (i.e. the long leg of the comb filter is a simple FIFO).

The digital system has additional flexibility in that FIR filter components can be uploaded to the FPGA and be used for channel equalization. This equalization can convolve out the effects of, for example, dispersion in cables and high power amplifiers.

The specific implementation of the digital part of the wideband feedback system is depicted in Figure 14.

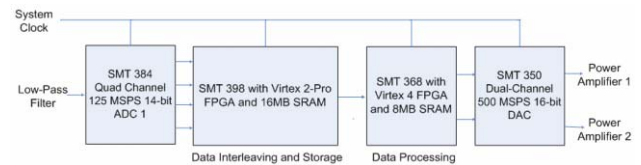


Figure 14: Digital implementation of feedback system. Photo courtesy of Schulte.

Figure 14 shows that the FPGA based system has dual outputs for driving the power amplifiers. The input is a SMT 384 ADC module and uses four interleaved 14 bit a/d converters that can run up to 125 MHz each, making the overall system capable of running at up to 500 MSa/sec. A picture of the a/d card is shown in Figure 15.

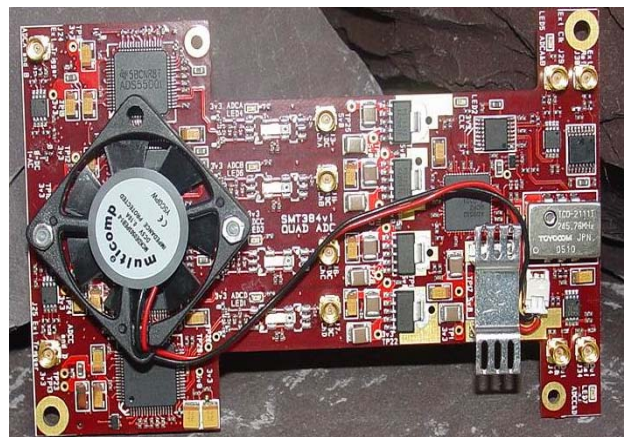


Figure 15: SMT 384 ADC module. Photo courtesy of Sundance DSP.

After the data is taken using the module in Figure 15, the data is sent to another FPGA card where it is then interleaved into a single data stream using another FPGA module, the SMT 398 developed by Sundance DSP. A photo of this board is shown in Figure 16. This card has been the greatest challenge in the entire system design as the routing on the FPGA is critical for the system data to be timed in or clocked properly.



Figure 16: SMT 398 module. Photo courtesy of Sundance DSP.

The next card in the chain of FPGAs is the SMT 368 module. This module contains all of the specifics of the facility and hardware, namely the delays, FIR coefficients, and types of comb filters. All of the DSP for the system and specialized programming for the wideband feedback system is done on this card. A picture of this card is shown in Figure 17.



Figure 17: SMT 368 module. Photo courtesy of Sundance DSP.

The final stage to the FPGA based system is shown in Figure 18. This stage is slated to change soon as it is a SMT 350 DAC module. This is the d/a converter and it interpolates data at up to 500 MSa/sec down to 125 MSa/sec. A replacement of this card to a true 500 MSa/sec DAC is planned.

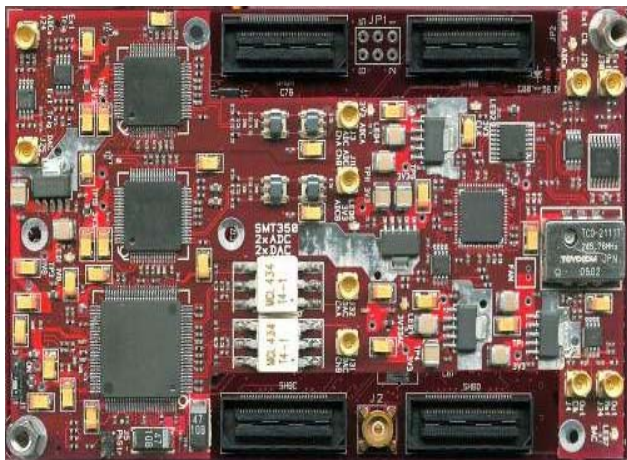


Figure 18: SMT 350 DAC module. Photo courtesy of Sundance DSP.

The block diagram of the digital programming for the FPGA system of Figure 17 is shown in Figure 19.

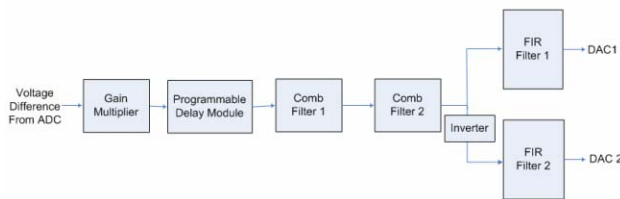


Figure 19: The system has a programmable gain, delay, FIR filter, two comb filters and outputs for each power amplifier.

Each part of the system can be bypassed and not change the overall delay through the system. This permits the system to be operationally flexible. The inputs and outputs are stored to on-board high-speed memory, which is 4 million 16 bit numbers deep.

CONCLUSION

We have shown that the e-p instabilities can be suppressed by an analog electronics, but it has limitations. It is desired to make a more robust system that can be flexible and keep its clock synchronized to the ring RF system as accumulation takes place. Designs of the new system are underway..

REFERENCES

- [1] D. Neuffer et al., "Observations of a fast transverse instability in the PSR", NIM A321, p. 1(1992).
- [2] R. Macek et al., "Electron Proton Two-Stream Instability at the PSR", Proceedings of the 2001 Particle Accelerator Conference, p. 688(2001).
- [3] R. Macek et al., "Test of a prototype active damping system for the e-p instability at the LANL PSR," paper TUAX04, Proceedings of HB2006, Tsukuba, Japan, May 29 - June 2, 2006.
- [4] S. Cousineau et al., "Experimental Observations and Simulations of Electron-Proton Instabilities in the Spallation Neutron Source Ring," International Workshop on Electron-Cloud Effects; Daegu, Korea, April 9 -12, 2007.
- [5] C. Deibele et al., "Design and Implementation of an Analog Feedback Damper System for an Electron-Proton Instability at the Los Alamos Proton Storage Ring," EPAC 2006, THPCH130.
- [6] A. Poliseti et al., "De-embedding a Cable Using FIR Signal Processing Techniques," <http://it.sns.ornl.gov/asd/public/pdf/sns0171/sns0171.pdf>.